PERGAMON

Vision Research 41 (2001) 1459–1474

Vision Research

www.elsevier.com/locate/visres

Sustained extrastriate cortical activation without visual awareness revealed by fMRI studies of hemianopic patients

Rainer Goebel [a,*], Lars Muckli [b], Friedhelm E. Zanella [c], Wolf Singer [b], Petra Stoerig [d]

[a] *Department of Cognitive Neuroscience, Faculty of Psychology, Maastricht University, Postbus 616, NL-6200MD Maastricht, The Netherlands*
[b] *Max Planck Institute for Brain Research, Deutschordenstr. 46, D-60528 Frankfurt a. M., Germany*
[c] *Klinikum der Johann Wolfgang Goethe-Universität, Institut für Neuroradiologie, 60528 Frankfurt a. M., Germany*
[d] *Institute of Experimental Psychology II, Heinrich-Heine-University, Universitätsstr.1, D-40225 Düsseldorf, Germany*

Received 23 January 2001; received in revised form 15 February 2001

Abstract

Patients with lesions in the primary visual cortex (V1) may show processing of visual stimuli presented in their field of cortical blindness even when they report being unaware of the stimuli. To elucidate the neuroanatomical basis of their residual visual functions, we used functional magnetic resonance imaging in two hemianopic patients, FS and GY. In the first experiment, a rotating spiral stimulus was used to assess the responsiveness of dorsal stream areas. Although no response was detectable within denervated or destroyed early visual cortex, motion-sensitive areas (hMT + /V5) ipsilateral to the lesion showed a strong sustained hemodynamic response. In GY, this activation was at least as strong as that of his contralesional hMT + /V5 to the stimulus in the normal hemifield. In the second experiment, coloured images of natural objects were used to assess the responsiveness of ventral stream areas. Again, no activity was detectable in ipsilesional early visual areas, but extrastriate areas in the lateral occipital cortex (hMT + /V5 and LO) and within the posterior fusiform gyrus (V4/V8) showed a robust sustained hemodynamic response. In both experiments, we observed that ipsilesional areas responded to stimuli presented in either hemifield, whereas the normal hemisphere responded preferentially to stimuli in the sighted hemifield. As only one subject occasionally noticed the onset of stimuluation in the impaired field, the unexpectedly strong sustained activity in ipsilesional dorsal and ventral cortical areas appears to be insufficient to generate conscious vision.

Keywords: Cortical blindness; Blindsight; Hemianopia; Visual cortical areas; Visual awareness; fMRI; Lesion

1. Introduction

The term 'blindsight' describes the ability of neurological patients with postgeniculate lesions to detect, localise and discriminate visual stimuli in blind parts of the visual field, although they do not consciously perceive them (Weiskrantz, Warrington, Sanders, & Marshall, 1974). These residual visual functions must be mediated by those parts of the visual system that retain visual responsiveness despite the lesion that destroys or denervates primary visual cortex (V1) and causes cortical blindness. Data from monkeys have shown that despite retrograde degeneration of projection cells in the dorsal lateral geniculate nucleus (dLGN) and the retina (Van Buren, 1963; Cowey, Stoerig, & Perry, 1989), subcortical retinorecipient nuclei continue to receive visual input from the parts of the retinae that represent the cortically blind visual field (for a recent review, see Stoerig & Cowey, 1997). Some of these nuclei project directly to extrastriate visual cortex, which consists of cytoarchitectonically distinct areas that subserve specific visual functions (Zeki, 1974; Zilles & Clarke, 1997). Evidence indicates that these areas are organized within two main visual pathways (Mishkin, Ungerleider, & Macko, 1983): a ventral stream or 'what' system devoted to the fine-grained analysis of the visual scene, including processing of shape and colour and a dorsal stream or 'where' system, which processes spatial characteristics of the visual scene and analyses motion. Emphasizing that the latter pathway is also involved in visuomotor transformations, Milner and

* Corresponding author. Tel.: +49-69-96769471; fax: +49-69-96769327.
E-mail address: r.goebel@psychology.unimaas.nl (R. Goebel).

0042-6989/01/$ - see front matter
PII: S0042-6989(01)00069-4

Goodale (1995) proposed to distinguish between 'vision for perception' (ventral pathway) and 'vision for action' (dorsal pathway). The two pathways originate in areas V1 and V2 and extend into the temporal (the 'what' system) and parietal (the 'where' system) lobe, respectively. With brain imaging techniques, they have been convincingly demonstrated in the normal human brain (e.g. Haxby et al., 1991) and several specialized areas have been identified on the basis of their stimulus preference profiles.

An extensively studied area in the ventral stream is area V4, which in the macaque, appears to be involved in the processing of chromatic and shape information (see Cowey, 1994 for a review). It has been reported to mediate colour constancy, but nevertheless, its necessity for colour vision is debated on the grounds that ablation of this area does not produce marked deficits in colour discrimination (Heywood & Cowey, 1987). In man, the colour complex has been located in the fusiform gyrus (Lueck et al., 1989; Hadjikhani, Liu, Dale, Cavanagh, & Tootell, 1998), in a region that is generally compromised in patients with achromatopsia (Meadows, 1974) and is often referred to as V4 (McKeefry & Zeki, 1997; Zeki, McKeefry, Bartels, & Frackowiak, 1998) or V8 (Hadjikhani et al., 1998); we shall refer to it here as the 'colour complex' or V4/V8. Other areas located in close proximity to area V4/V8 have been characterized, including the fusiform face area (FFA, Kanwisher, Dermott, & Chun, 1997) and several overlapping regions sensitive to different object categories (e.g. Ishai, Ungerleider, Martin, Schouten & Haxby, 1999). Less specialized, with respect to object categories but responsive to common objects, abstract sculptures and famous faces is a more dorsal area in a region at the lateral-anterior aspect of the occipital lobe that Malach et al. (1995) called LO (lateral occipital complex).

Of the dorsal stream areas, those that are specialized for motion processing have received particular attention. In monkey cortex, the motion-selective area MT (middle temporal area) is located in the middle temporal sulcus, close to the junction of the occipital, temporal and parietal lobes (Van Essen, Maunsell & Bixby, 1981). Its cells are responsive to the direction and speed of moving stimuli (Snowden, Treue & Andersen, 1992) and their inactivation causes deficiencies in motion direction discrimination. Area MT is easily identified in histological sections because of its high myelination and it is surrounded by several other specialized areas ('satellites') that process higher-order aspects of stimulus motion. The human visual cortex contains an area that is likely to correspond to monkey area MT and is located in the occipito-temporo-parietal pit. Bilateral lesions, that include this area, cause a severe impairment in detecting the movement of objects (cortical akinetopsia, see Zeki, 1991). Imaging studies have shown that metabolism and blood flow in that region increases more in response to moving than to stationary stimuli, indicating preferential involvement of this area in the processing of motion information (e.g. Watson et al., 1993; Tootell et al., 1995; Goebel, Khorram-Sefat, Muckli, Hacker, & Singer, 1998a). As functional imaging studies have not yet convincingly differentiated between the human homologue of area MT and its satellites, this motion-selective region is generally referred to as the 'human motion complex' (hMT+) or as V5.

Although area MT receives its major input directly or indirectly from the primary visual cortex (V1), destruction or temporary inactivation of V1 in monkeys does not eliminate its visual responsiveness (Rodman, Gross & Albright, 1989). Although the responses were markedly reduced, a large part of the neuronal population remained visually responsive and even retained directional tuning. Accordingly, one might expect residual visual responsiveness in the motion complex of human patients who have suffered lesions to the primary visual cortex, and indeed, functional imaging studies in patients with lesions of the optic radiation or primary visual cortex have confirmed its continued responsiveness to moving or flickering stimuli (Barbur, Watson, Frackowiak, & Zeki, 1993; Stoerig, Goebel, Muckli, Hacker, & Singer, 1997; Zeki & ffytche, 1998). In contrast to dorsal stream areas, neurons in the monkey's ventral stream become unresponsive to stimuli in the blind field after V1 lesions (Girard, Salin & Bullier, 1991; Bullier, Girard & Salin, 1993). Thus, one would expect little, if any, activity in areas of the ventral stream in patients with lesions to the primary visual cortex. However, in a recent imaging study of two hemianopic patients, we have found that presentation of images of natural objects in the cortically blind visual field can lead to strong sustained activity in the ventral pathway without any detectable activity in primary visual cortex (Goebel et al., 1998b; Goebel, Muckli, Zanella, Singer, & Stoerig, submitted).

In the present study, we compare the responsiveness of dorsal and ventral (Goebel et al., submitted) stream areas after blind field stimulation in the two hemianopic patients, GY and FS, as measured by echoplanar functional magnetic resonance imaging. To activate dorsal stream areas, a rotating spiral stimulus was presented in the cortically blind visual field. We used a rotating spiral instead of translational motion (Sahraie et al., 1997; Zeki & ffytche, 1998) because it restricts motion to a limited region of space for prolonged stimulation epochs (e.g. 30 s). This allowed us to separate the hemodynamic response to stimulus onset, which GY can be aware of (see Barbur, Ruddock, & Waterfield, 1980) from the sustained response to the rotatory motion. For activation of ventral stream areas, coloured images of natural objects (fruit and vegetables) were

used (Goebel et al., submitted). Both stimulus types were also presented in the sighted visual field of the patients to allow for a direct within-subject comparison of the hemodynamic response to stimulation in the cortically blind and in the intact visual field. As a further control, the same experiments were conducted with two healthy subjects. In addition, retinotopic mapping experiments were performed to describe the precise spatial layout of the functional responsiveness of early visual areas in the normal and lesioned hemisphere.

2. Methods

2.1. Patients

FS and GY, who participated in this study, have long-standing post-geniculate lesions of the left hemisphere (see Fig. 1). FS, born in 1937, suffered a severe craniocerebral trauma when he was 42 years of age. GY, born in 1956, was involved in a traffic accident when he was 8 years, and his left primary visual cortex was almost completely destroyed by a vascular incident. The visual field defects that resulted from the lesions are shown in Fig. 2. The wedge-shaped region in FS's right hemifield (black) is absolutely blind, while GY's hemianopia is relative and allows conscious detection of salient visual events. Over many years, GY and FS have participated in studies of their residual visual functions (e.g. for GY: Barbur et al., 1980; Blythe, Bromley, Kennard, & Ruddock, 1986; Brent, Kennard, & Ruddock, 1994; Weiskrantz, Barbur, & Sahraie, 1995; Morland, Ogilvie, Ruddock, & Wright, 1996; Finlay, Jones, Morland, Ogilvie, & Ruddock, 1997; Marcel, 1998; Guo, Benson, & Blakemore, 1998; Benson, Guo, & Blakemore, 1998; Kentridge, Heywood, & Weiskrantz, 1999 and for FS: Pöppel, 1985, 1986; Stoerig, 1993; Stoerig & Cowey, 1997; Stoerig, Kleinschmidt, & Frahm, 1998).

The lesions were visualized by MR-imaging (Fig. 1) using a high-resolution T1-weighted 3D FLASH sequence (voxel size $1 \times 1 \times 1$ mm) recorded with a 1.5 T scanner (Siemens Magnetom Vision). FS's extensive lesion primarily affects the temporal lobe and includes the optic radiation in the vicinity of the LGN. In GY, the medial occipital lobe of the left hemisphere is destroyed, including most of V1, as well as surrounding extrastriate visual cortex and the underlying white matter, but sparing the occipital pole.

2.2. Tasks

2.2.1. Retinotopic mapping

The responsiveness and delineation of early visual areas V1, V2, V3, VP, V3A, V4v and V4d was investigated with retinotopic mapping scans (cf. Sereno, Dale, Reppas, Kwong, Belliveau, Brady, Rosen, & Tootell, 1995), sampling 12 contiguous slices approximately in parallel to the calcarine fissure. Eccentricity and polar angle mapping experiments were performed in the same recording session (for details see Linden, Kallenbach, Heinecke, Singer, & Goebel, 1999). For eccentricity mapping, a ring-shaped configuration of black and white contrast-reversing (8 Hz) checkers was presented centered around the fixation point. The ring started with a radius of 1° visual angle and expanded to a radius of 12° within 96 s. For polar angle mapping, the same pattern was configured as a wedge subtending 22.5° in polar angle with the tip at the fixation cross. The wedge started at the left horizontal meridian and slowly rotated clockwise for a full cycle of 360° within 96 s. Each mapping experiment consisted of four repetitions of a full expansion and a full rotation.

2.2.2. Mapping of the motion complex

Motion-selective areas were identified by comparing the hemodynamic response during presentation of a moving stimulus with the response during presentation of a stationary control stimulus. We used a flowfield stimulus, consisting of 400 white dots moving radially outward on a black background (visual field: 28° wide by 20° high, dot size: 0.06×0.06°, dot velocity: 3.6–14.4°/s). It was contrasted with a stationary dot display to produce a clear response of motion-sensitive areas (Tootell et al., 1995).

2.2.3. Motion experiment (Experiment 1)

While the flowfield stimulated both hemifields simultaneously, the main stimulus was presented 6.8° off-axis in one hemifield at a time. It consisted of a blue-and-red (run 1) or black-and-white (run 2) checkered spiral (Fig. 2A,C), 7° in diameter, rotating counter-clockwise around its centre (180°/s). Each stimulation block lasted for 30 s and was repeated four times within each run. In an additional condition, a stationary spiral was shown four times in four blocks of 30 s. All stimulation blocks were separated by fixation blocks of equal length. The stimulus was presented on a grey background to prevent light scatter from the stimulus into the sighted hemifield. A schematic drawing of the stimulus configuration is shown in Fig. 2(A,C).

2.2.4. Object experiment (Experiment 2)

Coloured images of natural objects (fruit and vegetables) subtending 5.2×5.2° were presented in the left (normal) or right (impaired) upper visual field, 7° off-axis (Fig. 2B). Each stimulation block lasted for 30 s and was repeated four times within each recording session. Stimulation blocks were separated by fixation blocks of equal length. Within a stimulation block, an image was shown for 1 s and then replaced by the next image without an interstimulus interval. Images con-

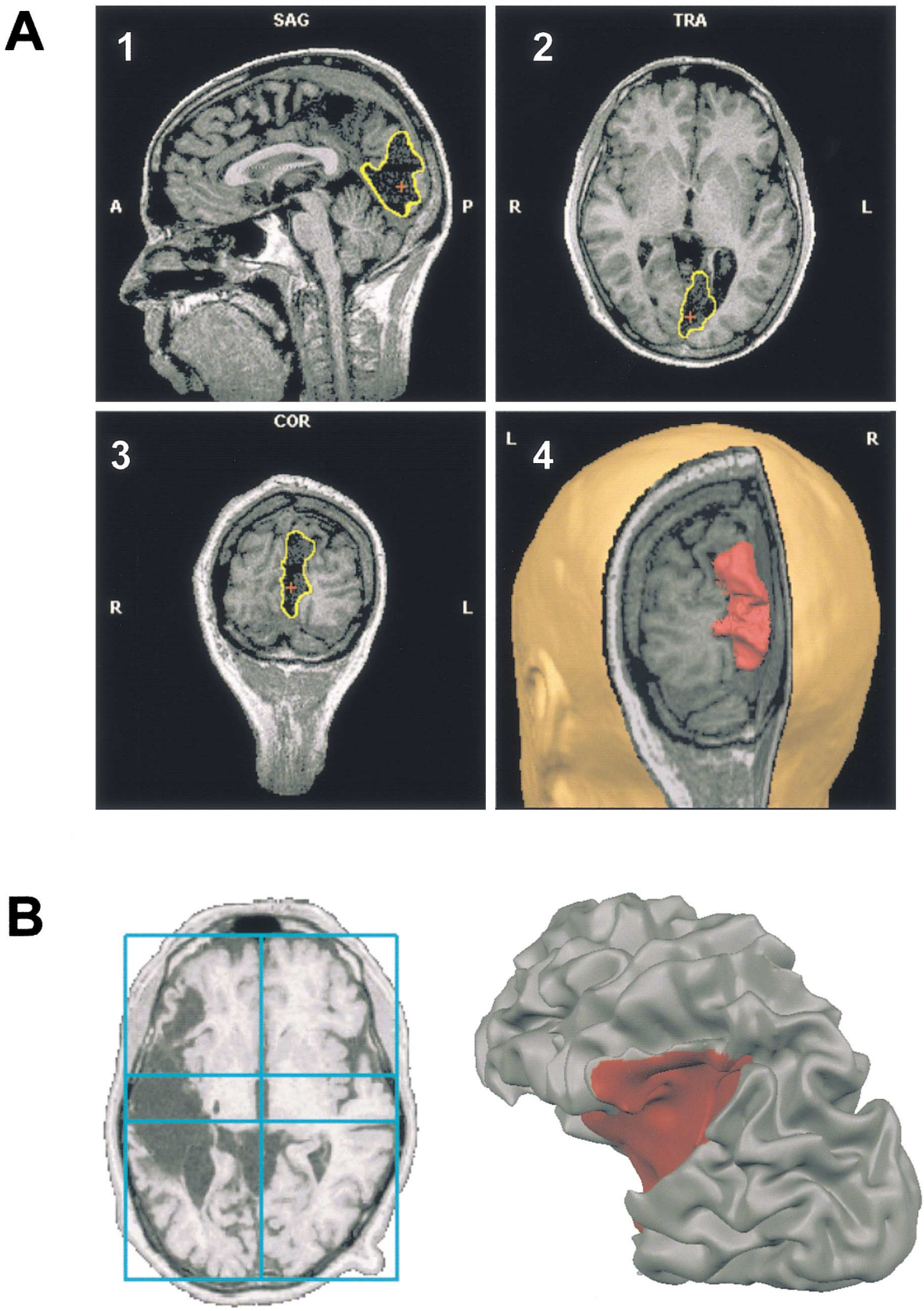

Fig. 1. Lesions of patients GY (A) and FS (B). (A) Slices of an anatomical T1-weighted MRI scan showing the V1 lesion of GY. The small cross in (1–3) indicates the 3D position of the selected slices, the yellow curve delineate the extend of the lesion within the respective slices. (1) Sagittal slice through the lesion. (2) Axial slice through the lesion. (3) Coronal slice through the lesion. (4) Surface rendering of GYs reconstructed head (yellow) and of the boundary of the V1 lesion (red). The rendered head was partially opened to reveal the size and position of the lesion. (B) Rendering of the reconstructed cortical surface at the boundary between grey and white matter of the affected left hemisphere of patient FS. An image containing a single slice running through the lesion is also shown.

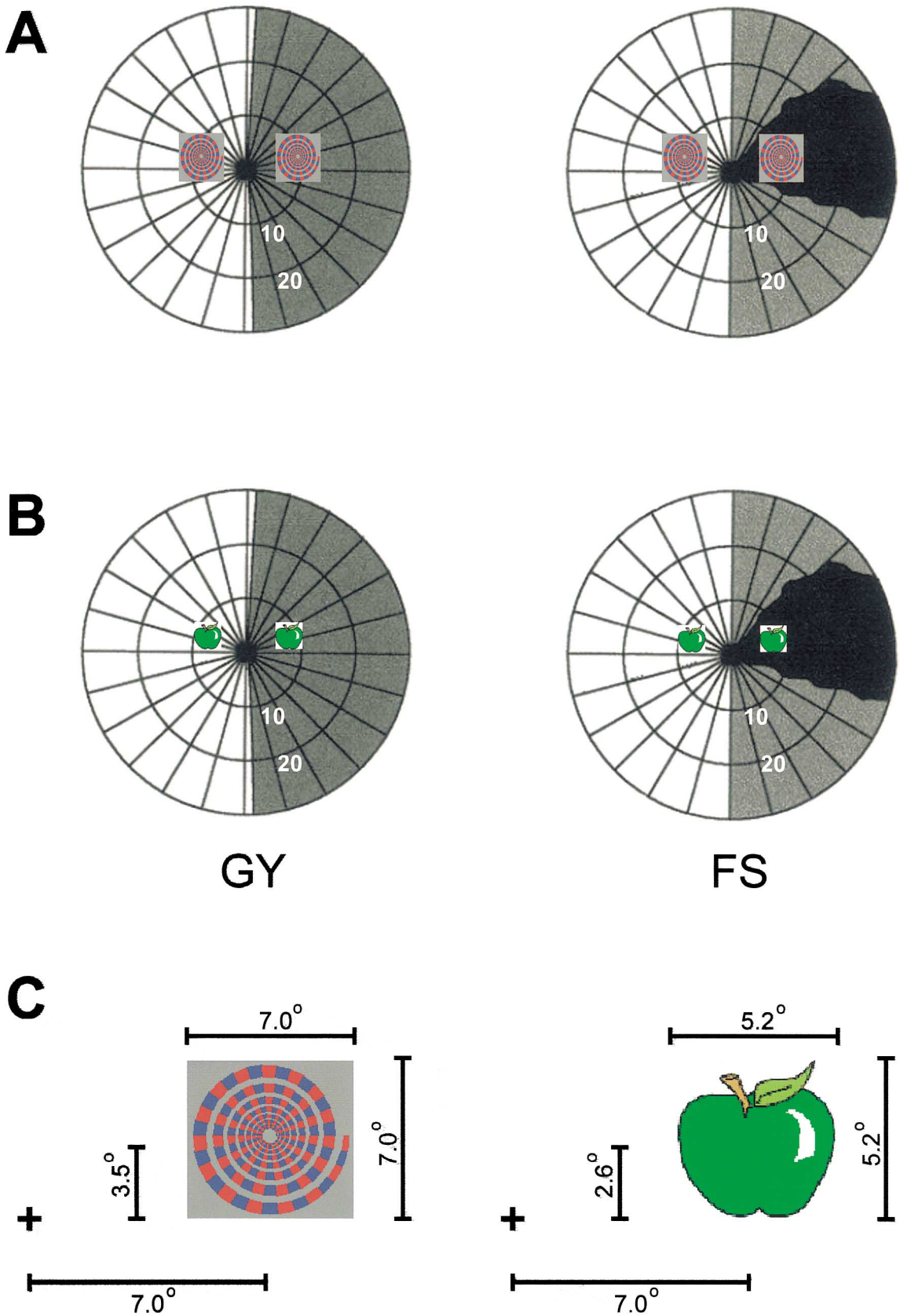

Fig. 2. Plots of visual field sensitivity (A,B) which are based on a combination of static and dynamic perimetry (target: 116', 320 cyc deg^{-1} m^{-2}, background: 10 cyc deg^{-1} m^{-2}; white: normal field, black: absolutely blind field; grey: relatively blind region, see text). (A) Visual field sensitivity plot with indicated position of the moving spiral stimulus for GY (left) and FS (right). (B) Visual field sensitivity plot with indicated stimulation position in the objects experiment for GY (left) and FS (right). Stimuli were shown in separate blocks in either the left or the right visual field. (C) Stimulus size and location in the spiral experiment (left) and in the objects experiment (right).

sisted of coloured drawings of natural objects (fruit and vegetables, Corel Draw clip art gallery). The stimuli were presented on a white background to minimize stray light falling into the sighted hemifield. A schematic drawing of the stimulus configuration is shown in Fig. 2(B,C).

In order to assess whether the subjects were aware of the stimuli presented in the cortically blind hemifield, we asked them to respond by button press when they detected anything in the right visual hemifield.

2.3. MRI acquisition

Functional magnetic resonance imaging was performed at 1.5 T (Siemens Magnetom Vision) using the standard head coil and a gradient echo EPI sequence. The Siemens Magnetom gradient overdrive allowed functional scans with high spatial and temporal resolution (TE = 69 ms, TR = 3000 ms, FA = 90°, FOV = 200×200 mm^2, matrix size: 128×128, voxel size: $1.6 \times 1.6 \times 3$–5 mm^3). A T1-weighted 3D MP RAGE scan lasting 8 min was performed in the same session (voxel size $1 \times 1 \times 1$ mm^3). An additional T1-weighted 3D data set tuned to optimize the contrast between gray and white matter was recorded in a separate recording session lasting 24 min (FLASH sequence). The intrasession MP RAGE 3D data set was automatically aligned with the extrasession T1 FLASH data set. Visual stimuli were delivered under computer control (Digital DECpc Celebris XL 590) to a high-luminance LCD projector (EIKI LC-6000). The image was back-projected onto a frosted screen positioned at the foot of the scanner. Visual stimuli were generated using the Microsoft DirectX graphics library and a Matrox Mystique graphics board.

2.4. Data analysis

FMRI data analysis was performed using BrainVoyager 3. × /2000 (Brain Innovation, Maastricht, The Netherlands, www.BrainVoyager.com) and included removal of low-frequency drifts, 3D motion detection and correction, determination of Talairach coordinates, multiple regression analysis, cortex reconstruction, inflation and flattening. For the retinotopic mapping experiments, cross-correlation analysis was applied (for details see Linden et al., 1999). The eccentricity and polar angle represented by a given cortical site was determined by finding the lag value maximizing the cross-correlation. The obtained lag values at each voxel, corresponding to the eccentricity or polar angle of optimal stimulation, were encoded in pseudocolours on slices as well as on surface patches (triangles) of the reconstructed cortical sheet (see below). Pixels were included into the statistical map if the obtained cross-correlation value r was > 0.4 ($P < 0.0001$, uncorrected). In order to detect weak activity within and surrounding the lesioned or denervated regions, retinotopic mapping experiments were also analysed with a lowered correlation threshold of $r > 0.2$. Based on the polar angle, mapping the boundaries of retinotopic cortical areas V1, V2, V3, VP, V3A and V4v were estimated on the flattened cortical surface maps (see below) of each patient's non-lesioned hemisphere and of both hemispheres in each control subject. The motion complex mapping experiment was analysed with a simple correlation analysis contrasting the flowfield stimulus with the stationary control stimulus.

The two main experiments were analysed with a multiple regression model consisting of two predictors, one for the presentation of the stimulus (moving spiral/images of natural object) in the left and one for the presentation of the stimulus in the right visual field. The overall model fit was assessed using an F statistic. The obtained P-values were corrected for multiple comparisons using a cortex-based Bonferroni adjustment, i.e. the number of voxels included for correction was limited to grey matter voxels (Goebel & Singer, 1999). The relative contribution of each of the two predictors $RC = (b_1 - b_2)/(b_1 + b_2)$ was visualised with a red-yellow-green pseudocolour scale. Statistical maps were superimposed on the original functional scans and incorporated into the high-resolution 3D MRI data sets through interpolation to the same resolution (voxel size: $1 \times 1 \times 1$ mm). Since the 2D functional and 3D structural measurements were acquired in the same recording session, coregistration of the respective data sets could be performed on the basis of the Siemens slice position parameters of the T2*-weighted measurement (number of slices, slice thickness, distance factor, TraCor angle, FOV, shift mean, offcenter read, offcenter phase, in-plane resolution) and the T1-weighted 3D MP RAGE measurement (number of sagittal partitions, shift mean, offcenter read, offcenter phase, resolution). In order to compare activated brain regions across sessions, anatomical and functional 3D data sets were transformed into Talairach space (Talairach & Tournaux, 1988). Results were visualised by superimposing 3D statistical maps on reconstructions of each patient's cortical sheet. Areas were identified based on their anatomical position and Talairach coordinates.

The recorded high-resolution T1-weighted 3D recordings were used for surface reconstruction of both cortical hemispheres of the control subjects and patients (for details see Linden et al., 1999; Kriegeskorte & Goebel, submitted). The white/grey matter border was segmented with a region-growing method preceded by inhomogeneity correction of signal intensity across space. The border of the resulting segmented subvolume was tessellated to produce a polygon-mesh surface reconstruction of each cortical hemisphere. The tessellation of the white/grey matter boundary of a single

hemisphere typically consists of ≈ 250000 triangles. An iterative 3D morphing algorithm (Goebel et al., 1998a) was used to move the vertices outward along the surface normals into the grey matter. Through visual inspection, this process was halted when the surface reached the middle of the gray matter corresponding approximately to layer 4 of the cortex. The resulting surface was used as the reference mesh for projecting functional data on folded, inflated or flattened representations. A morphed surface was always linked to its folded reference mesh, so that functional data could be shown at the correct location of an inflated or flattened representation. This link was also used to minimize geometric distortions during inflation and flattening (Goebel, 2000) by inclusion of a morphing force that keeps the distances between vertices of each triangle of the morphed surface as close as possible to the respective values of the folded reference mesh.

3. Results

Results from a control subject of the retinotopic mapping, motion complex mapping and objects experiment are shown in Fig. 3. Results of the two patients are shown in Figs. 4–6.

3.1. Retinotopic mapping

The topography of the early visual areas is shown in Fig. 3(A) for a normal observer. In the patients, the contralesional V1 appeared normal, but no visual responsiveness was seen in its lesioned (GY) or denervated (FS) counterpart ($r \geqq 0.4$, $P < 0.00001$). Only a small region at the occipital pole was activated in GY (Fig. 5(A), see also Baseler, Morland, & Wandell, 1999). This is in agreement with GY's visual field perimetry that shows a 3° macular sparing in the lower quadrant of the hemianopic right visual field (Barbur et al., 1980).

3.2. Motion complex mapping

The comparison of the flowfield stimulus with the stationary dot stimulus revealed several motion-selective areas in both hemispheres including the motion complex, area V3A and an area at the border between occipital and parietal lobes (Fig. 3B). In GY, the motion complex in the ipsilesional hemisphere is located more posteriorly and more ventrally than in the contralesional hemisphere. The position of the motion complex in both patients (Table 1) agrees with previous reports in normal observers (Tootell et al., 1995; Goebel et al., 1998a).

3.3. Motion experiment

In the control subjects, the foci of activation in the lateral occipital cortex produced by passive viewing of the moving spiral were functionally identified as hMT + /V5 because they overlapped with the regions activated by the flowfield stimulus (not shown). When the moving spiral stimulus was presented in the cortically blind (right) visual field of the patients, the ipsilesional (left) motion complex was strongly activated (Fig. 4) despite the fact that there was no detectable activation within and around the lesioned or denervated region. A weaker but significant response was also observed in the contralesional motion complex. When the spiral stimulus was presented in the left (sighted) hemifield, both the contralesional motion complex, as well as the ipsilesional motion complex, responded strongly (see Fig. 4). Thus, the motion complex at the ipsilesional side responded equally strong (FS) or stronger (GY) to the moving spiral presented in the cortically blind visual field, whereas the response of the contralesional motion complex was stronger to the spiral in the sighted (left) visual field in both patients.

In $< 20\%$ of the presentations of the rotating spiral in the cortically blind hemifield, GY pressed the button for a short duration following the onset of the spiral, indicating that he was aware of a stimulus change. An analysis of the data restricted to the first 15 s of the 30-s stimulation epochs produced almost identical results as the analysis restricted to the last 15 s. FS never indicated awareness when stimuli were presented in his blind visual field.

In GY, the comparison of the hemodynamic response to the presentation of the moving spiral in the cortically blind visual field and the sighted visual field revealed that the extent of the functionally defined motion complex in the lesioned hemisphere was greater than in the intact hemisphere (Table 2). Interestingly, this difference was more pronounced in the black-white spiral experiment than in the red-blue spiral experiment. The red-blue spiral, although not isoluminant, possessed much less luminance contrast than the black-white spiral. We quantified the observation of an extended ipsilesional motion complex in GY using the number of activated voxels as well as the maximal correlation values in the obtained statistical maps (Table 2). During presentation of the moving spiral in the cortically blind visual field, the maximum single-voxel correlation value was $r_{\max} = 0.62$ (black-white spiral) and $r_{\max} = 0.61$ (red-blue spiral) and located in the ipsilesional motion complex. With a fixed single-voxel correlation value of $r > 0.4$ ($P < 0.00001$, uncorrected), the cluster size (CS = number of activated voxels) was $CS_{r>0.4} = 93$ (black-white spiral) and $CS_{r>0.4} = 61$ (red-blue spiral). During presentation of the moving spiral in the

sighted visual hemifield, the maximum single-voxel correlation value was $r_{max} = 0.55$ (black-white spiral) and $r_{max} = 0.60$ (red-blue spiral) and located in the contralesional motion complex. With a value of $CS_{r>0.4} = 40$, the cluster size was also larger for the red-blue than the black-white spiral ($CS_{r>0.4} = 26$), indicating that in the normal hemisphere, chromatic contrast is more effective than in the lesioned one.

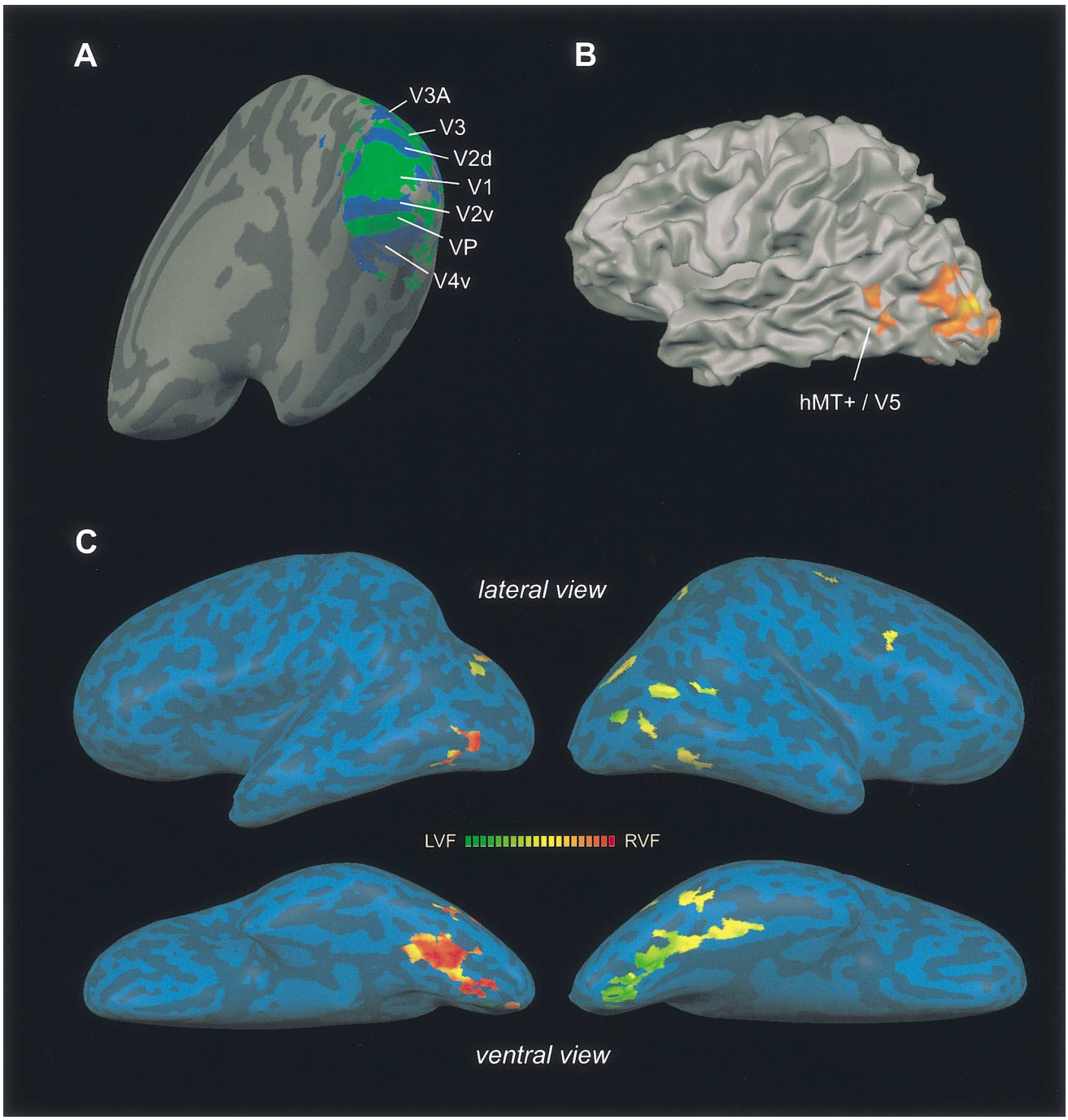

Fig. 3. Results of a control subject of the retinotopic mapping experiment (A), motion complex mapping experiment (B) and objects experiment (C). (A) Boundaries of retinotopic cortical areas were determined through field sign map computations (cf. Sereno et al., 1995) based on eccentricity and polar angle mapping. (B) Lateral view of the reconstructed cortical sheet. The statistical map comparing the flowfield condition with the stationary dots condition is projected on the surface revealing motion-selective areas including V3A and hMT + /V5. (C) Lateral and ventral view of 'inflated' cortical hemispheres. Activated regions responding solely to objects presented in the left visual field are coloured green; regions responding solely to objects presented in the right visual field are coloured red. Areas responding with equal strength to stimuli in either hemifield are shown in yellow (for graded values, see colour scale).

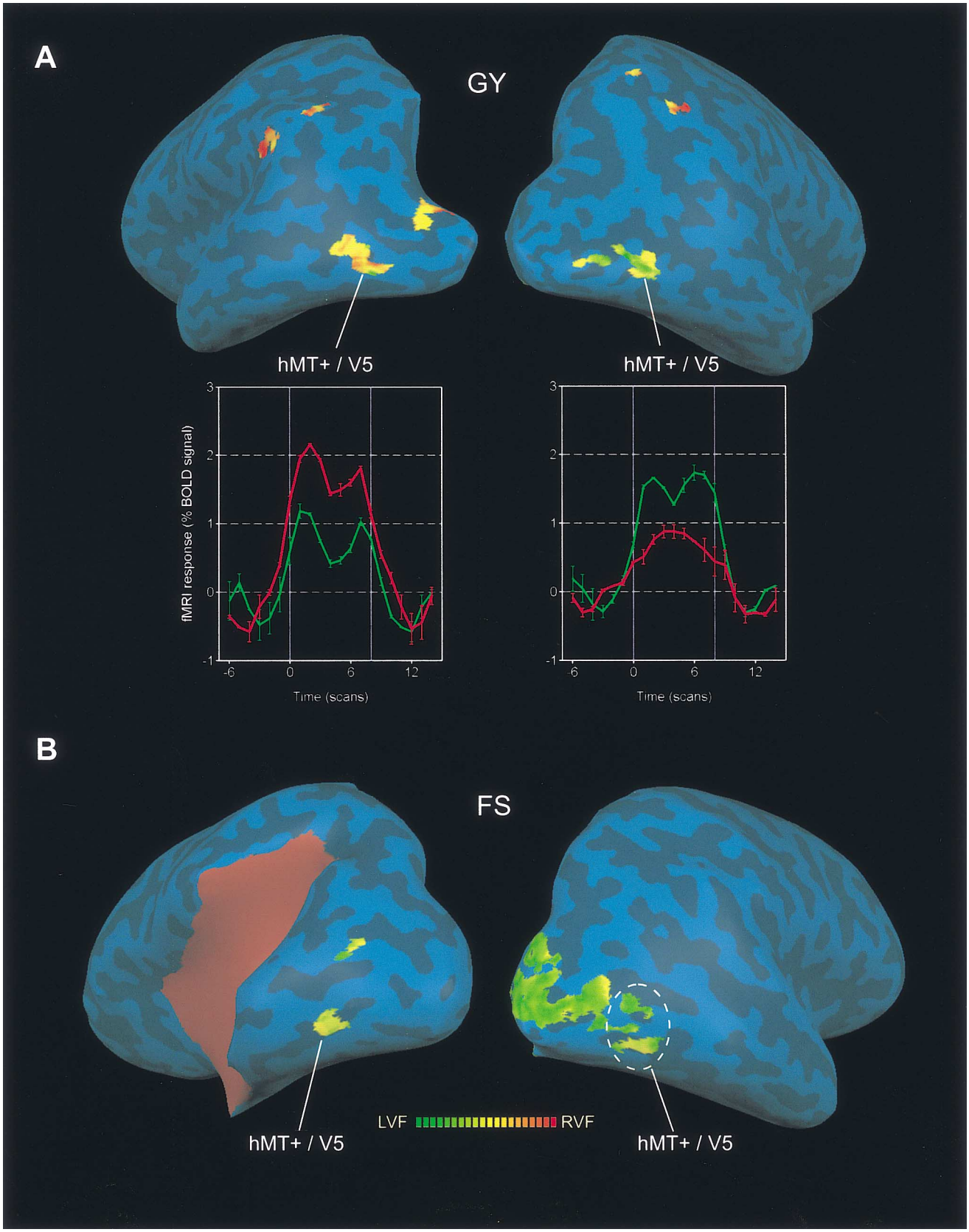
A
GY
hMT+ / V5
hMT+ / V5
fMRI response (% BOLD signal)
3
2
1
0
-1
-6
0
6
12
Time (scans)
3
2
1
0
-1
-6
0
6
12
Time (scans)
B
FS
LVF
RVF
hMT+ / V5
hMT+ / V5

Fig. 4.

3.4. Object experiment

In the control subjects, activated regions in early visual areas responded solely to objects presented in the contralateral visual field (Fig. 3C). With increasing distance from V1, visual areas responded also to stimuli in the ipsilateral visual field as indicated in Fig. 3(C) by the change from red to yellow color (left hemisphere) and green-to-yellow color (right hemisphere). Regions responding equally well to stimuli in both visual fields (yellow) were more extended in the right hemisphere. The human motion complex, which is known to respond not only to motion but also to flickering stimuli (Tootell et al., 1995) also responded strongly to the presentation of the images. The motion complex in either hemisphere responded to stimuli in both visual fields albeit with a stronger response to the respective contralateral hemifield.

The normal hemisphere in the patients responded to stimuli in the normal hemifield with a similar activation pattern as that seen in the control subjects, and includes early visual areas, the lateral occipital cortical region and a region in the fusiform gyrus (Fig. 5(B) and Fig. 6(B), right hemisphere). Activity in the lesioned hemisphere caused by stimuli in the normal field (Fig. 5(B,C) and Fig. 6(B,C), green curves) was less extended than in the controls, but in GY, the region in the fusiform gyrus responded as well as it did to stimuli in the normal hemifield. Much to our surprise, ventral areas in the lesioned hemishere responded quite strongly to images presented in the impaired (right) hemifield (Fig. 5C and Fig. 6C, red curves),. In GY, both a region in the fusiform gyrus and the lateral occipital region were activated. These foci presumably correspond to V4/V8 and area LO, respectively, as their Talairach coordinates (Table 1) closely match those reported in the literature (Malach et al., 1995; Hadjikhani et al., 1998). Time courses show that the ipsilesional response strength in area V4/V8 is nearly the same for stimuli in the blind and sighted field, but the response of area LO is weaker for stimuli in the blind field (Fig. 5C). In FS, the lateral occipital region in the lesioned hemisphere responded roughly half as strong to images in the impaired hemifield compared to the response after sighted field stimulation (Fig. 6C), but there was only little activation in V4/V8. In both subjects, some activation was also seen in hMT+/V5. In GY, bilateral hMT+/V5 activity was observed after stimulation in either hemifield (Fig. 5B,C), but in FS, only stimulation of the normal hemifield elicited bilateral hMT+/V5; no significant activity was observed after stimulation in the blind visual field (Fig. 6B,C). Throughout, the normal hemisphere showed very little activation in response to stimuli in the impaired field, indicating that the coactivation of corresponding areas commonly seen in higher extrastriate cortical areas is compromised. In contrast to control subjects, no activity was observed anterior to V4/V8 in the left, lesioned hemisphere in either patient.

In $<10\%$ of the presentations of the objects in the cortically blind hemifield, GY pressed the button for a short duration following the onset of the image sequence, indicating that he was aware of a stimulus change. An event-related analysis of 'aware' versus 'unaware' epochs produced almost identical results. As in the motion experiment, FS never indicated awareness when stimuli were presented in his blind visual field.

Table 1
Talairach coordinates (x, y, z) of regions hMT+/V5, LO, and V4/V8 in the left (LH) and right (RH) hemisphere of patients GY and FS.

	GY LH	GY RH	FS LH	FS RH
hMT+/V5	−36, −67, 1	47, −63, 0	−48, −76, 0	47, −64, −3
LO	−39, −73, −15	45, −65, −20	−38, −67, −8	43, −65, −16
V4/V8	−25, −65, −12	22, −62, −21	−35, −62, −18	28, −53, −17

Table 2
Two measures characterizing the response strenght in hMT+/V5 in the left, lesioned hemisphere after blind field stimulation and in the right hemisphere after stimulation in the sighted hemifield: maximum observed correlation value (r_{max}) and cluster size (number of connected, activated pixels) at a specified correlation value of $r = 0.4$ ($CS_{r=0.4}$)

	Black-white spiral		Red-blue spiral	
	r_{max}	$CS_{r=0.4}$	r_{max}	$CS_{r=0.4}$
RH	0.55	26	0.60	40
LH	0.62	93	0.61	61

Fig. 4. Multiple regression results of the black-and-white spiral experiment of patient GY (A) and patient FS (B), shown on inflated representation of the cortical sheet. Activated regions responding solely to the spiral presented in the left visual field are coloured green; regions responding solely to the spiral presented in the right visual field are coloured red. Areas responding with equal strength to the spiral in either hemifield are shown in yellow (for graded values, see colour scale). (A) Activated regions in the right hemisphere are dominated by green colors whereas regions in the lesioned left hemisphere are dominated by yellow colors. The extent of the functionally defined motion complex is greater in the ipsilesional hemisphere than in the intact hemisphere. Time courses of left and right hemispheric motion complex (hMT+/V5) for left hemifield stimulation (green curves) and right hemifield stimulation (red curves). (B) Activated regions in the right hemisphere are dominated by green colors whereas regions in the lesioned left hemisphere are dominated by yellow colors.

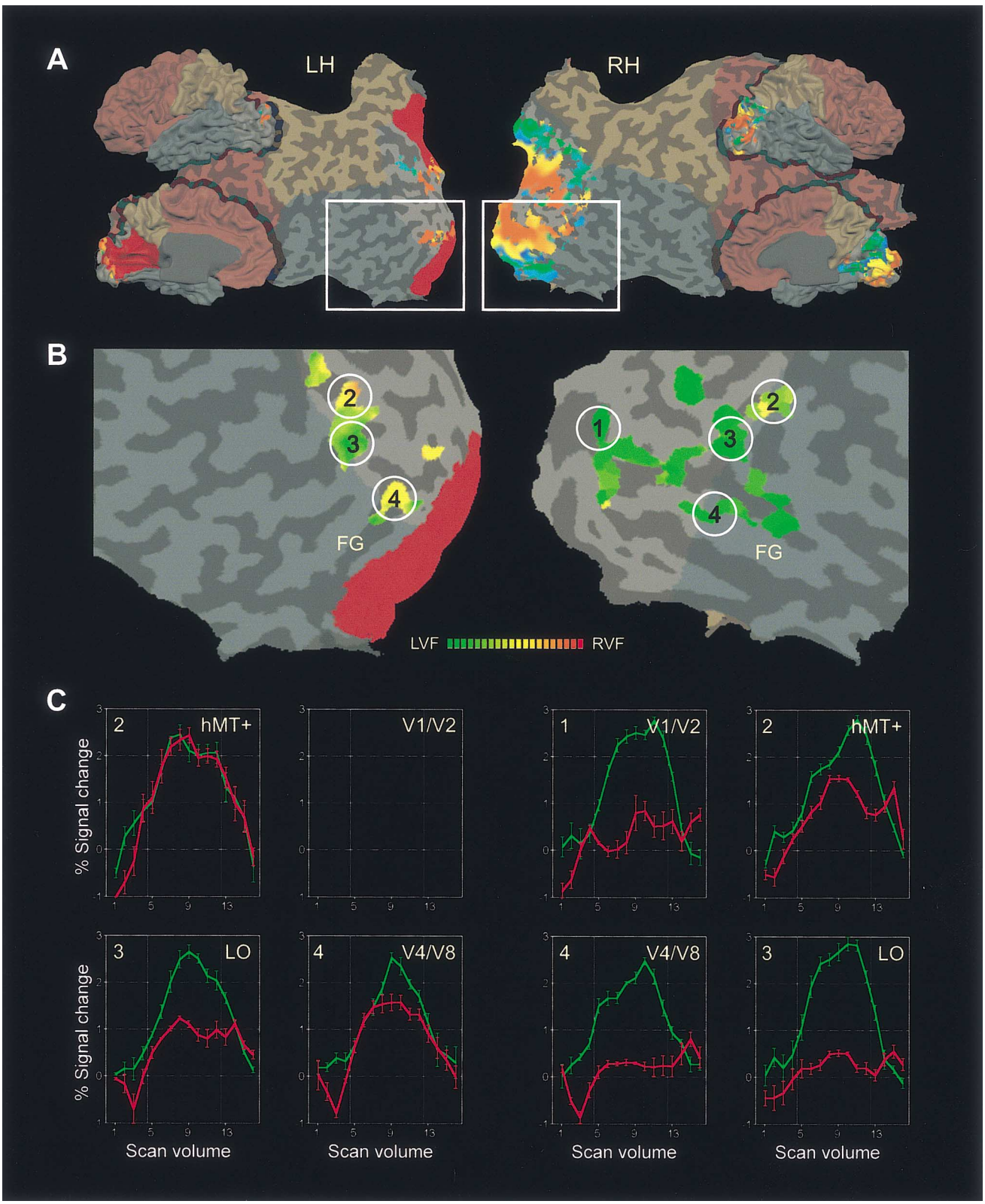

Fig. 5. Multiple regression results of object experiment of patient GY. Dark red regions in (A) and (B) correspond to the boundary of the cortex and the lesion; LH = left hemisphere, RH = right hemisphere. (A) Folded (small insets) and flattened representation of the reconstructed cortical sheet with superimposed results of eccentricity mapping; foveal to peripheral visual field representations are coded in colour from red to yellow to blue to green. (B) Results of the object experiment superimposed on a subpart of the flattened cortex representation of each hemisphere as indicated with white rectangles in (A). Activated regions responding solely to objects presented in the left visual field are coloured green, regions responding solely to objects presented in the right visual field are coloured red. Areas responding with equal strength to stimuli in either hemifield are shown in yellow (for graded values, see colour scale); FG = fusiform gyrus. (C) Time courses of right hemispheric area V1/V2 and left and right hemispheric areas hMT + /V5, presumed LO and presumed V4/V8 for left hemifield stimulation (green curves) and right hemifield stimulation (red curves); location of plotted areas are indicated by numbers 1–4 in (B).

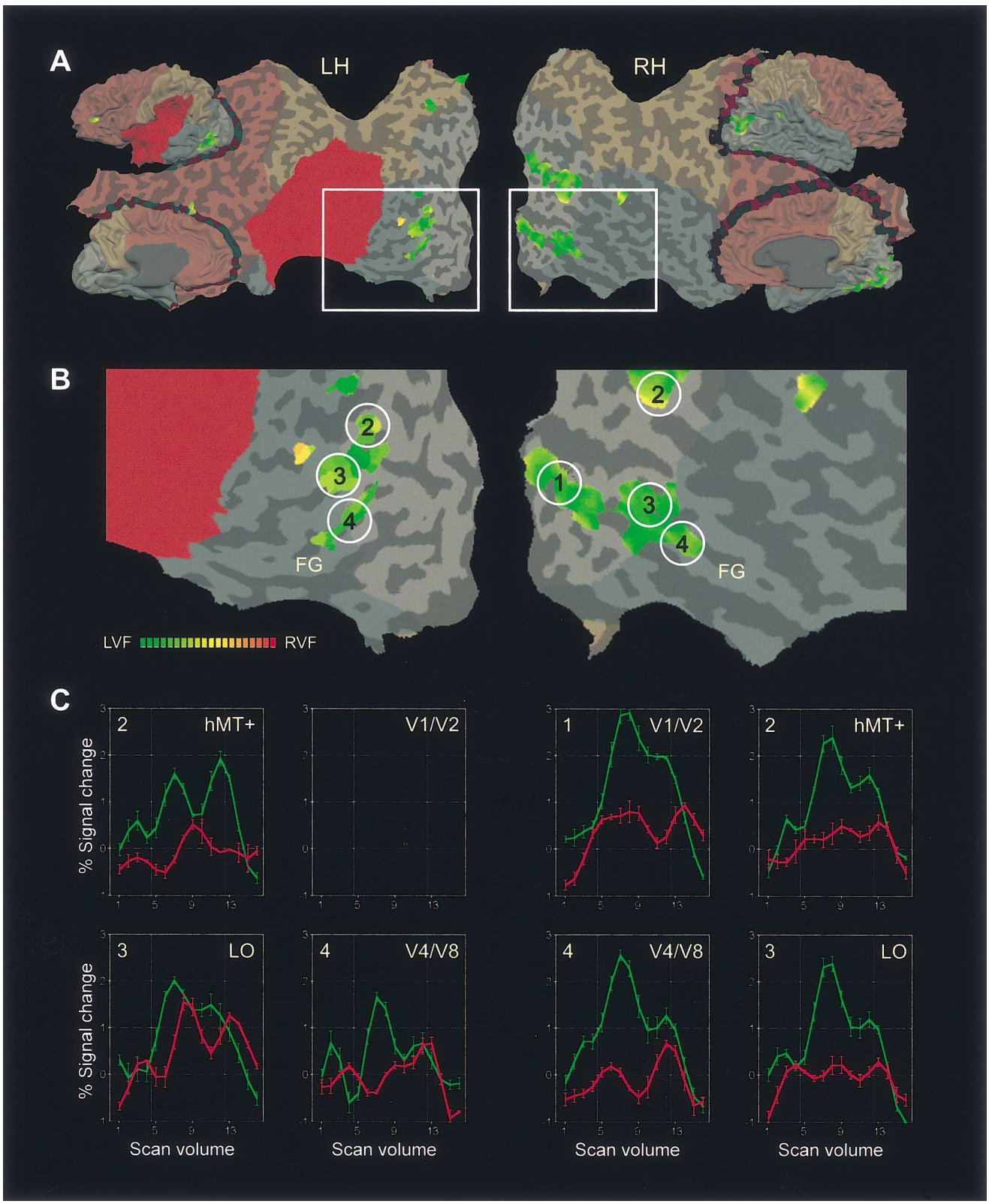

Fig. 6. Multiple regression results of object experiment of patient FS. Dark red regions in (A) and (B) correspond to the boundary of the cortex and the lesion; LH = left hemisphere, RH = right hemisphere. (A) Folded (small insets) and flattened representation of the reconstructed cortical sheet with superimposed results of the main experiment. (B) Results of the object experiment superimposed on a subpart of the flattened cortex representation of each hemisphere as indicated with white rectangles in (A). Activated regions responding solely to objects presented in the left visual field are coloured green, regions responding solely to objects presented in the right visual field are coloured red (for graded values, see colour scale); FG = fusiform gyrus. (C) Time course plots of areas of interest as in Fig. 5; location of plotted areas are indicated by numbers 1–4 in (B).

4. Discussion

4.1. Summary

We studied activation patterns in dorsal and ventral cortical areas in response to a rotating spiral and to images of natural objects presented in the intact and cortically blind fields of two hemianopic patients. We found surprisingly strong responses to blind-field stimulation in ipsilesional extrastriate areas including the motion complex, but also in ventral areas, which probably correspond to area LO and V4/V8. There was no detectable activity in the early visual cortical areas of the lesioned hemisphere and with the exception of GY's occasional button press at stimulus onset, the patients indicated no awareness of the stimuli. In addition, the data revealed an unexpected asymmetry: the areas of the intact hemisphere responded well to stimulation of the contralateral, sighted hemifield but very little to stimulation of the impaired hemifield. In contrast, the corresponding areas in the lesioned hemisphere responded to stimulation of either hemifield.

4.2. Extrastriate cortical activation without V1

A strong and sustained activity in extrastriate areas is not what one would have expected on the basis of previous monkey experiments which showed that responses of neurons in MT, while still present, are markedly reduced (Rodman et al., 1989) and that neurons in ventral stream areas become unresponsive to visual stimuli presented in the affected hemifield (Girard et al., 1991; Bullier et al., 1993). It appears unlikely that the observed activation is mediated by only partially damaged V1 tissue (Fendrich, Wessinger, & Gazzaniga, 1992; Wessinger, Fendrich, & Gazzaniga, 1997) since several other functional imaging studies have also shown an absence of detectable activation in the lesioned cortex in GY (see Barbur et al., 1993; Sahraie et al., 1997; Zeki & ffytche, 1998; Baseler, Morland, & Wandell, 1999; Kleiser, Wittsack, Niedeggen, Goebel, & Stoerig, 2001) and the denervated region in FS (Stoerig et al., 1998; Kleiser et al., 2001) after blind field stimulation. Nevertheless, of the two findings, the dorsal activation of hMT+ is less surprising. It has been reported before (Barbur et al., 1993; Sahraie et al., 1997; Stoerig et al., 1997; Zeki & ffytche, 1998) and it agrees well with psychophysical data showing that 'dorsal' functions, such as localization (Pöppel, Frost & Held, 1973; Weiskrantz et al., 1974) and motion processing (Barbur et al., 1980; Pöppel, 1985; Blythe et al., 1986; Perenin, 1991; Benson et al., 1998) can be demonstrated in cortically blind fields. In view of the physiological results from monkey studies (Rodman, Gross & Albright, 1990), it is likely that the information reaches hMT+ via the colliculo-pulvino-extrastriate cortical pathway. What is unexpected is the extent of ipsilesional hMT+ activation in GY, which, different from FS, is actually as pronounced as that of the motion complex in the intact hemisphere when it is stimulated from the normal hemifield. The strength of activation runs counter the reduction seen in the physiological data from monkeys with ablated or cooled V1 and may indicate plastic changes of the system compensating for the loss of V1 which is normally the major (direct and indirect) source of hMT+ input. When compared to FS, in whom the activation was weaker on the lesioned side, one may suggest that GY's much earlier lesion allowed for better reorganization. That it is luminance rather than chromatic contrast that reveals the extent of GY's hMT+ activation could be seen as a consequence of the degenerative effects of a V1 lesion on the colour-opponent retino-geniculo-striate cortical system that originates in the Pβ-ganglion cells of the retina (Cowey et al., 1989): The magnocellular luminance- and motion-processing system feeding into the dorsal pathway is much less compromised.

In view of the data from monkeys, whose V1 had been deactivated (Bullier et al., 1993), the activation of ventral cortical areas from stimulation of the impaired field is most unexpected. In the absence of V1, the information could reach the ventral areas either via direct subcortical projections, as those from the degenerated lateral geniculate nucleus (Yukie & Iwai, 1981; Cowey & Stoerig, 1989), or it could arise via lateral dorso-ventral connections. Our data do not allow refutation of either hypothesis, although the latter is rendered somewhat less likely by the weakness of the object-induced activity seen in hMT+. Preliminarily, we have attributed this hMT+ activation to the image presentation frequency of 1 Hz which represents a slow flicker. 'Ventral' functions, such as chromatic (Pöppel, 1986; Stoerig, 1987; Stoerig & Cowey, 1992; Brent et al., 1994) and shape discrimination (Weiskrantz et al., 1974; Weiskrantz, 1987; Marcel, 1998; Stoerig, in preparation, 1998) have also been demonstrated in cortically blind visual fields, although they are generally more difficult to elicit than the dorsal functions, and require more testing to reveal weaker, albeit sometimes highly significant, results. Our results indicate that it may be the human colour complex V4/V8 that mediates the residual processing of chromatic information, as chromatic information activates this region (Lueck et al., 1989; Hadjikhani et al., 1998) and its destruction entails achromatopsia (Meadows, 1974). This assumption fits well with findings showing good chromatic processing in GY (Brent et al., 1994 Barbur et al., 1999 Stoerig, in preparation), but poorer processing in FS (Stoerig, 1987; in preparation) whose V4/V8 was not detectably activated during blind field stimulation. The ipsilesional lateral occipital area LO that responded in both subjects could be involved in residual form pro-

cessing, although the psychophysical predictions suggested by the response properties of LO — better response to objects than textures, comparable responses to faces, objects, and abstract sculptures (Malach et al., 1995), and reduction of activity in response to scrambled natural objects (Grill-Spector et al., 1998) — have not yet been tested.

4.3. Asymmetry of extrastriate cortical activation

While we found that each hemisphere was activated by its contralateral visual hemifield, activation by the ipsilateral hemifield was asymmetrical for the two hemispheres. Though this pattern was less obvious in dorsal areas, the ventral foci of the intact hemisphere responded much less to stimulation of the impaired hemifield than did those of the lesioned hemisphere to stimulation of the normal hemifield. In addition, the activation in the lesioned ventral areas is quite focal: it does not extend forward or backward as it does in the intact hemisphere. It is possible that these extrastriate areas, while able to respond to stimuli in the impaired field, are incapacitated with respect to conveying activity forward, backward, or to the other hemisphere. Such an inability to effectively transmit signals to other areas might be caused by inactivation of recurrent loops between higher and early visual areas. Recurrent loops can organize neuronal activity into stable resonant states, which have been proposed as the neural correlate of conscious vision (e.g. Tononi & Edelman, 1998; Grossberg, 1999; Engel & Singer, 2001). As we found sustained and pronounced cortical activity in both subjects without awareness of the presented stimuli, our data are in agreement with such 'resonance' theories, but not with simple 'activation threshold theories' (Palmer, 1999), which assume that any cortical neural activity sufficiently strong or lasting will produce conscious experience of the content it represents.

Acknowledgements

It is a pleasure to thank FS and GY for participation in this study. We thank Claudia I. Goebel for her help in performing this study and Niko Kriegeskorte for helpful comments on the manuscript. This work was supported by the Max Planck Society and a Human-Capital and Mobility network grant from the European Community.

References

Barbur, J. L., Ruddock, K. H., & Waterfield, V. A. (1980). Human visual responses in the absence of the geniculo-calcarine projection. *Brain*, *103*, 905–928.

Barbur, J. L., Watson, J. D., Frackowiak, R. S., & Zeki, S. (1993). Conscious visual perception without V1. *Brain*, *116*, 1293–1302.

Baseler, H. A., Morland, A. B., & Wandell, B. A. (1999). Topographic organization of human visual areas in the absence of input from primary cortex. *Journal of Neuroscience*, *19*, 2619–2627.

Benson, P. J., Guo, K., & Blakemore, C. (1998). Direction discrimination of moving gratings and plaids and coherence in dot displays without primary visual cortex (V1). *European Journal of Neuroscience*, *10*, 3767–3772.

Blythe, I. M., Bromley, J. M., Kennard, C., & Ruddock, K. H. (1986). Visual discrimination of target displacement remains after damage to the striate cortex in humans. *Nature*, *320*, 619–621.

Brent, P. J., Kennard, C., & Ruddock, K. H. (1994). Residual colour vision in a human hemianope: spectral responses and colour discrimination. *Proceedings of the Royal Society London. Series B: Biology Science*, *256*, 219–225.

Bullier, J., Girard, P., & Salin, P.-A. (1993). The role of area 17 in the transfer of information to extrastriate visual cortex. In A. Peters, & K. S. Rockland, *Cerebral cortex*, vol. 10 (pp. 301–330). New York: Plenum Press.

Cowey, A. (1994). Cortical visual areas and the neurobiology of higher visual processes. In M. J. Farah, & G. Ratcliff, *The Neuropsychology of high-level vision* (pp. 3–31). Hillsdale, NJ: Lawrence Erlbaum.

Cowey, A., & Stoerig, P. (1989). Projection patterns of surviving neurons in the dorsal lateral genicualte nucleus following discrete lesions of striate cortex: implications for residual vision. *Experimental Brain Research*, *75*, 631–638.

Cowey, A., Stoerig, P., & Perry, V. H. (1989). Transneuronal retrograde degeneration of retinal ganglion cells after damage to striate cortex in macaque monkeys: selective loss of P beta cells. *Journal of Neuroscience*, *29*, 65–80.

Engel, A. K., & Singer, W. (2001). Temporal binding and the neural correlates of sensory awareness. *Trends in Cognitive Sciences*, *5*, 16–25.

Fendrich, R., Wessinger, C. M., & Gazzaniga, M. S. (1992). Residual vision in a scotoma. Implications for blindsight. *Science*, *258*, 1489–1491.

Finlay, A. L., Jones, S. R., Morland, A. B., Ogilvie, J. A., & Ruddock, K. H. (1997). Movement in the normal visual hemifield induces a percept in the 'blind' hemifield of a human hemianope. *Proceedings of the Royal Society London. Series B*, *264*, 267–275.

Girard, P., Salin, P. A., & Bullier, J. (1991). Visual activity in macaque area V4 depends on area 17 input. *Neuroreport*, *2*, 81–84.

Goebel, R. (2000). A fast automated method for flattening cortical surfaces. *NeuroImage*, *11*, S680 Abstract.

Goebel, R., & Singer, W. (1999). Cortical surface-based statistical analysis of functional magnetic resonance imaging data. *NeuroImage*, *9*, S64 Abstract.

Goebel, R., Khorram-Sefat, D., Muckli, L., Hacker, H., & Singer, W. (1998a). The constructive nature of vision: direct evidence from functional magnetic resonance imaging studies of apparent motion and motion imagery. *European Journal of Neuroscience*, *10*, 1563–1573.

Goebel, R., Stoerig, P., Muckli, L., Zanella, F. E., & Singer, W. (1998b). Ipsilesional visual activation in ventral extrastriate cortex in patients with blindsight. *Social Neuroscience Abstracts*, *24*, 1508.

Goebel, R., Muckli, L, Zanella, F.E., Singer, W. & Stoerig, P. (submitted). Sustained activation without visual awareness in ipsilesional ventral cortical areas of hemianopic patients.

Grill-Spector, K., Kushnir, T., Hendler, T., Edelman, S., Itzchak, Y., & Malach, R. (1998). A sequence of object-processing stages revealed by fMRI in the human occipital lobe. *Human Brain Mapping*, *6*, 316–328.

Grossberg, S. (1999). The link between brain learning, attention, and consciousness. *Conscious Cognition*, *8*, 1–44.

Guo, K., Benson, P. J., & Blakemore, C. (1998). Residual motion discrimination using colour information without primary visual cortex. *NeuroReport*, *9*, 2103–2106.

Hadjikhani, N., Liu, A. K., Dale, A. M., Cavanagh, P., & Tootell, R. B. H. (1998). Retinotopy and color sensitivity in human visual cortical area V8. *Nature Neuroscience*, *1*, 235–241.

Haxby, J. V., Grady, C. L., Horwitz, B., Ungerleider, L. B., Mishkin, M., Carson, R. E., Herscovitch, P., Schapiro, M. B., & Rapoport, S. I. (1991). Dissociation of spatial and object visual processing pathways in human extrastriate cortex. *Proceedings of the Natural Academy of Science USA*, *88*, 1621–1625.

Heywood, C. A., & Cowey, A. (1987). On the role of cortical area V4 in the discrimination of hue and pattern in macaque monkeys. *Journal of Neuroscience*, *7*, 2601–2617.

Ishai, A., Ungerleider, L. G., Martin, A., Schouten, J. L., & Haxby, J. V. (1999). Distributed representation of objects in the human ventral visual pathway. *Proceedings of the Natural Academy of Science USA*, *96*(16), 9379–9384.

Kanwisher, N., McDermott, J., & Chun, M. M. (1997). The fusiform face area: a module in human extrastriate cortex specialized for face perception. *Journal of Neuroscience*, *17*, 4302–4311.

Kentridge, R. W., Heywood, C. A., & Weiskrantz, L. (1999). Effects of temporal cueing on residual visual discrimination in blindsight. *Neuropsychologia*, *37*, 479–483.

Kleiser, R., Wittsack, J., Niedeggen, M., Goebel, R. & Stoerig, P. (2001). Is V1 necessary for conscious vision in areas of relative cortical blindness? NeuroImage, in press.

Kriegeskorte, N. & Goebel, R. (submitted). An efficient algorithm for topologically correct segmentation of the cortical sheet in anatomical MR volumes.

Linden, D. E. J., Kallenbach, U., Heinecke, A., Singer, W., & Goebel, R. (1999). The myth of upright vision. A psychophysical and functional imaging study of adaptation to inverting spectacles. *Perception*, *28*, 469–481.

Lueck, C. J., Zeki, S., Friston, K. J., Deiber, M. P., Cope, P., Cunningham, V. J., Lammertsma, A. A., Kennard, C., & Frackowiak, R. S. (1989). The colour centre in the cerebral cortex of man. *Nature*, *340*, 386–389.

Malach, R., Reppas, J. B., Benson, R. R., Kwong, K. K., Jiang, H., Kennedy, W. A., Ledden, P. J., Brady, T. J., Rosen, B. R., & Tootell, R. B. (1995). Object-related activity revealed by functional magnetic resonance imaging in human occipital cortex. *Proceedings of the Natural Academy of Science USA*, *92*, 8135–8139.

Marcel, A. J. (1998). Blindsight and shape perception: deficit of visual consciousness or of visual function? *Brain*, *121*, 1565–1588.

McKeefry, D. J., & Zeki, S. (1997). The position and topography of the human colour centre as revealed by functional magnetic resonance imaging. *Brain*, *120*, 2229–2242.

Meadows, J. C. (1974). Disturbed perception of colours associated with localized cerebral lesions. *Brain*, *97*, 615–632.

Milner, A. D., & Goodale, M. A. (1995). *The visual brain in action*. Oxford: Oxford University Press.

Mishkin, M., Ungerleider, L. G., & Macko, K. A. (1983). Object vision and spatial vision: two cortical pathways. *Trends in Neuroscience*, *6*, 414–417.

Morland, A. B., Ogilvie, J. A., Ruddock, K. H., & Wright, J. R. (1996). Orientation discrimination is impaired in the absence of the striate cortical contribution to human vision. *Proceedings of the Royal Society London, Series B*, *263*, 633–640.

Palmer, S. E. (1999). *Vision science*. Cambridge, MA: MIT Press.

Perenin, M. T. (1991). Discrimination of motion direction in perimetrically blind fields. *Neuroreport*, *2*, 397–400.

Pöppel, E. (1985). Bridging a neuronal gap. Perceptual completion across a cortical scotoma is dependent on stimulus motion. *Naturwissenschaften*, *72*, 599–600.

Pöppel, E. (1986). Long-range colour-generating interactions across the retina. *Nature*, *320*, 523–525.

Pöppel, E., Frost, D., & Held, R. (1973). Residual visual function after brain wounds involving the central visual pathways in man. *Nature*, *243*, 295–296.

Rodman, H. R., Gross, C. G., & Albright, T. D. (1989). Afferent basis of visual response properties in area MT of the macaque. I. Effects of striate cortex removal. *Journal of Neuroscience*, *9*, 2033–2050.

Rodman, H. R., Gross, C. G., & Albright, T. D. (1990). Afferent basis of visual response properties in area MT of the macaque: 2. Effects of superior colliculus removal. *Journal of Neuroscience*, *10*, 1154–1164.

Sahraie, A., Weiskrantz, L., Barbur, J. L., Simmons, A., Williams, S. C. R., & Brammer, M. J. (1997). Pattern of neuronal activity associated with conscious and unconscious processing of visual signals. *Proceedings of the Natural Academy of Science USA*, *94*, 9406–9411.

Sereno, M. I., Dale, A. M., Reppas, J. B., Kwong, K. K., Belliveau, J. W., Brady, T. J., Rosen, B. R., & Tootell, R. B. H. (1995). Borders of multiple visual areas in humans revealed by functional magnetic resonance imaging. *Science*, *268*, 889–893.

Snowden, R. J., Treue, S., & Andersen, R. A. (1992). The response of neurons in areas V1 and MT of the alert rhesus monkey to moving random dot patterns. *Experimental Brain Research*, *88*, 389–400.

Stoerig, P. (1987). Chromaticity and achromaticity. Evidence for a functional differentiation in visual field defects. *Brain*, *110*, 869–886.

Stoerig, P. (1993). Spatial summation in blindsight. *Vision Neuroscience*, *10*, 1141–1149.

Stoerig, P. (in prep.) Apples and oranges: Discrimination of images of natural objects in patients with retro–geniculate lesions.

Stoerig, P., & Cowey, A. (1992). Wavelength discrimination in blindsight. *Brain*, *115*, 425–444.

Stoerig, P., & Cowey, A. (1997). Blindsight in man and monkey. *Brain*, *120*, 535–559.

Stoerig, P., Goebel, R., Muckli, L., Hacker, H., & Singer, W. (1997). On the functional neuroanatomy of blindsight. *Social Neuroscience Abstracts*, *23*, 845.

Stoerig, P., Kleinschmidt, A., & Frahm, J. (1998). No visual responses in denervated V1: high-resolution functional magnetic resonance imaging of a blindsight patient. *Neuroreport*, *9*, 21–25.

Talairach, J., & Tournaux, P. (1988). *Co-planar stereotaxic atlas of the human brain*. New York, NY: Thieme.

Tononi, G., & Edelman, G. M. (1998). Consciousness and complexity. *Science*, *282*, 1846–1851.

Tootell, R. B. H., Reppas, J. B., Kwong, K. K., Malach, R., Born, R. T., Brady, T. J., Rosen, B. R., & Belliveau, J. W. (1995). Functional analysis of human MT and related visual cortical areas using magnetic resonance imaging. *Journal of Neuroscience*, *15*, 3215–3230.

Van Buren, J. M. (1963). Trans-synaptic retrograde degeneration in the visual system of primates. *Journal of Neurology, Neurosurgery and Psychiatry*, *34*, 140–147.

Van Essen, D. C., Maunsell, J. H. R., & Bixby, J. L. (1981). The middle temporal visual area in the macaque: myeloarchitecture, connections, functional properties and topographic organization. *Journal of Cognitive Neurology*, *201*, 81–98.

Watson, J. D. G., Myers, R., Frackowiak, R. S. J., Hajnal, J. V., Woods, R. P., Mazziotta, J. C., Shipp, S., & Zeki, S. (1993). Area V5 of the human brain: evidence from a combined study using positron emmission tomography and magnetic resonance imaging. *Cerebral Cortex*, *3*, 79–94.

Wessinger, C. M., Fendrich, R., & Gazzaniga, M. S. (1997). Islands of residual vision in hemianopic patients. *Journal of Comparative Neuroscience*, *9*, 203–221.

Weiskrantz, L. (1987). Residual vision in a scotoma. A follow-up study of 'form' discrimination. *Brain*, *110*, 77–92.

Weiskrantz, L., Warrington, E. K., Sanders, M. D., & Marshall, J. (1974). Visual capacity in the hemianopic field following a restricted occipital ablation. *Brain*, *97*, 709–728.

Weiskrantz, L., Barbur, J. L., & Sahraie, A. (1995). Parameters affecting conscious versus unconscious visual discrimination in a patient with damage to the visual cortex (V1). *Proceedings of the Natural Academy of Science USA*, *92*, 6122–6126.

Yukie, M., & Iwai, E. (1981). Direct projection from the dorsal lateral geniculate nucleus to the prestriate cortex in macaque monkeys. *Journal of Comparative Neurology*, *291*, 81–97.

Zeki, S. (1974). In R. G. E. G. Bellairs, *Essays on the nervous system — A festschrift for Professor J.Z. Young* (pp. 327–343). Oxford: Clarendon Press.

Zeki, S. (1991). Cerebral akinetopsia (visual motion blindness): a review. *Brain*, *114*, 811–824.

Zeki, S., & ffytche, D. H. (1998). The Riddoch syndrome: insights into the neurobiology of conscious vision. *Brain*, *121*, 25–45.

Zeki, S., McKeefry, D. J., Bartels, A., & Frackowiak, R. S. (1998). Has a new color area been discovered? *Nature Neuroscience*, *1*, 335–336.

Zilles, K., & Clarke, S. (1997). Architecture, connectivity, and transmitter receptors of human extrastriate visual cortex: comparison with nonhuman primates. In K. S. Rockland, J. H. Kaas, & A. Peters, *Cerebral cortex*, vol. 12 (pp. 673–742). New York: Plenum Press.